INTERPRETING MICRODOSIMETRIC SPECTRA

J. F. Dicello[1,2,3] and F. A. Cucinotta[4]

[1]Professor Emeritus of Radiation Oncology, Johns Hopkins University School of Medicine; [2][1]Professor of Radiation Medicine and Director of Biophysics, Loma Linda University Medical Center; [3]Visiting Research Professor, U.S. Naval Academy, [4]Chief Scientist, NASA, Space Radiation Program Element, Johnson Space Center

The field of microdosimetry is the study of those physical characteristics of energy transfers other than dose that produce variations in biological consequences of exposures to radiation. Historically, this area developed primarily from a need to understand and quantify the differences in human responses to different types of radiation, in particular the variations in late complications for the same level of acute effects such as edema and vomiting or tumor control in radiation therapy, and further applications in radiation health. In space applications, this field has been used to interpret variations in responses of personnel (and sometimes electronics) to the different radiation fields present in space environments, especially in comparison with exposures on the Earth's surface from which the preponderance of our radiobiological database originates. These variations result in differing risks which must be evaluated for the health and welfare of astronauts and for establishing compliance with regulatory limits. Research on the physical aspects of the radiations includes the investigation of probability density functions for energy transfers, molecular physics, track structure, thermodynamics, and even radiation chemistry as evidenced by the variety of articles published in the proceedings of the microdosimetry symposiums [Proceedings of the 15th International Symposium on Microdosimetry, 2011, and published proceedings of earlier symposiums] as well as other scientific literature [e.g., M. Zaider and J. F. Dicello, 2004 and references therein]. Again, scientists not in the field usually will encounter this area in terms of efforts to evaluate acute and late consequences of exposures or to determine levels of exposure for regulatory purposes [NCRP Report No. 137, (2001)]. The purpose of this article is to briefly present the fundamentals of the most common methods of presenting such data in the literature in order to briefly provide the casual reader sufficient background to better understand the data in context. To fulfill this objective, the article will focus on the most common method of presenting such data, i.e., probability distributions for energy deposited as a function of energy deposited, probability density functions, leaving the reader seeking further details to peruse more extensive publications such as NCRP 137 [2001].

We start by defining a few terms that we will use, some of which will be familiar and some of which will be esoteric [NCRP 137, 2001; Zaider and Dicello, 2004]

The dose, D, is defined as the energy, E, deposited per unit mass, m:

$$D = \Delta E / \Delta m \text{ (Gy)}. \qquad \text{Eq. 1}$$

where ΔE represents a small change approaching in the limit a mathematical differential, dE. However, dose is an average macroscopic quantity and should only be applied to sufficiently large volumes where equilibrium exists in the thermodynamic sense. To apply the term, then, to a single atom or a small number of units where statistical variations in energy deposition can be as much as four decades or more is usually nonsensical. Therefore, an analogous quantity for the energy deposited by events occurring in the statistical-mechanics regime of an ensemble of individual particles interacting within the microscopic and submicroscopic domains is defined as the specific energy, z. That is:

$$z = \frac{\varepsilon}{m} \ (Gy) \qquad\qquad\qquad\qquad \text{Eq. 2}$$

where ε is the energy deposited in a microscopic site of mass, m.

The energy lost per unit pathlength or linear energy transfer, L or LET, of a particle, sometimes called L_∞ because it includes all of the energy lost by the particle rather than only that fraction up to some specified cut-off, is defined as:

$$L = dE/dl \ (keV/\mu m) \qquad\qquad\qquad Eq.3$$

where l is a distance along the pathlength of the particle. LET also is another macroscopic quantity and should only be applied to large volumes where equilibrium exists in the thermodynamic sense. This should be readily apparent when the secondary electrons denoted as δ-rays produced by the particle can escape the volume when the particle traverses the volume or if δ-rays enter the volume originating from particles not traversing the volume. The LET is equivalent to the stopping power, dE/dx, of the particle, and, for a single particle of a specified energy, has a single value. LET values are frequently used in the evaluation of risks from radiation exposures.

We define a microscopic quantity analogous to the LET as the energy deposited by a single event in a volume of average or mean linear dimension, $\bar{l}$, as the lineal energy, y:

$$y = \frac{\varepsilon}{\bar{l}} \ (keV/\mu m) \qquad\qquad\qquad Eq. 4$$

To quantify expected differences in response for different radiations, energies, and/or biological endpoints, the Radiobiological Effectiveness, RBE is defined as:

$$RBE = Dcontrol/D_{unknown} \qquad\qquad\qquad Eq. 5$$

where $D_{unknown}$ is the dose of a radiation whose response is under investigation and $D_{control}$ is the dose of a control radiation of known response, usually x or gamma rays, that produce the same level of response. [Note that the RBE is <u>not</u> the ratio of the level of effects observed at a given dose.]

The dose equivalent, $D_{equivalent}$, is the dose of the radiation under investigation times the corresponding RBE and represents the dose of the control radiation that would have to be delivered to produce the same corresponding level of response.

$$D_{equivalent} = D_{unknown} \ x \ RBE = Dcontrol$$

Eq. 6

Quality Factor, Q, is one committee- or agency-determined equivalent of the RBE for protection purposes, needed because of the variations and gaps in data in order to establish uniformity in the determination of regulatory risks.
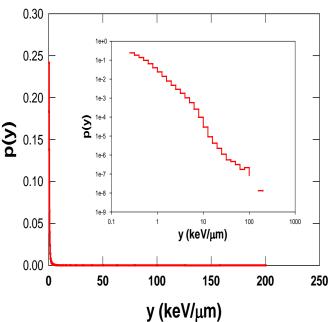
Risks and hazards, liberally used but frequently left undefined, are defined as follows:

A hazard is any external factor that can produce undesirable consequences. Risk refers either to the probability of producing an undesirable consequence or a quantity that is presumed proportional to that probability, such as the dose equivalent defined above. We define the probability of an occurrence of a specific type of event as the ratio of the number of such types of events divided by the total number of any type of events. As an example, the probability of an individual getting cancer is the number of individuals in a population getting cancer divided by the total number in the population. Probabilities therefore can vary between zero and 1 (100%).
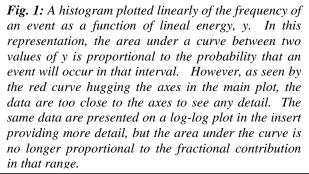
In microdosimetry, there are two probability functions that are frequently encountered, the probability of an event occurring with a lineal energy value of y, usually noted as p(y) or f(y), and the probability of a dose being deposited resulting from an event with lineal energy y, noted as d(y).

The hazard in the case of microdosimetry is usually radiation.   The consequences of radiation exposure can, for example, be cancer, coronary diseases, diseases of the central nervous system, and/or acute responses such as anemia at lower doses, vomiting, and even death at higher doses. (Controlled, local exposures also can result in the control of cancer and other diseases as well, although such consequences are called benefits rather than risks, and microdosimetric concepts are applicable to interpreting beneficial consequences as well.)

Now that the basic terminology is established, let us examine these concepts and quantities in terms of real spectra for different types of radiations, the types of representations seen in scientific publications.   In Figure 1 we start with a linear-linear histogram of the measured probability, p(y), of depositing a given amount

Fig. 1: *A histogram plotted linearly of the frequency of an event as a function of lineal energy, y. In this representation, the area under a curve between two values of y is proportional to the probability that an event will occur in that interval. However, as seen by the red curve hugging the axes in the main plot, the data are too close to the axes to see any detail. The same data are presented on a log-log plot in the insert providing more detail, but the area under the curve is no longer proportional to the fractional contribution in that range.*

of lineal energy, y, in a sphere of tissue-equivalent gas of 2-μm diameter embedded in tissue-equivalent plastic as a function of lineal energy. For this case, the sphere was irradiated with a therapeutic proton beam with a maximum energy of 250-MeV, with protons being the most common particle present in space environments [Dicello and Cucinotta, 2002].   One of the limitations of measured microdosimetric spectra is that the shape of the spectrum is dependent upon the size and shape of the target volume. A spherical volume is frequently chosen, because the pathlength distribution for randomly distributed straight tracks traversing a sphere is one of the simplest distributions, and it is independent of orientation in an external beam.   The average pathlength for this case is two-thirds of the diameter, presented here without proof [see Zaider and Dicello, 2004]. In this representation, the area under the curve between two values of lineal

energy, y, is proportional to the probability of events in that interval occurring. If the total area of the curve is normalized to one (100%), then the area between two values is the fractional contribution of events in that interval to the total number of events. Unfortunately, most distributions extend over several decades in lineal energy and as many as ten or more decades in probability, so the curves tend to hug the axes, as seen in Figure 1, and important details of the distributions are not seen. To demonstrate some of these salient features, we could plot the data as a histogram on a log-log basis, as demonstrated in the insert in Figure 1, but now the areas under the curve are no longer proportional to the fractional contributions in those intervals. We shall address this dilemma shortly, but first let us consider that the distribution in Figure 1 represents not only probability of an event occurring, but it is often the dose deposited by that event that is important in terms of the biological consequences, not the event *per se*. The dose that is deposited in the site is the sum of energies deposited by each event divided by the mass of the site or, equally, it is the probability that an event occurs time the energy deposited. Therefore (microscopic) specific dose deposited by an event having a lineal energy y is not p(y), the fraction of events within an interval Δy, but rather the fraction of events times the energy each deposits per unit mass. For a sphere of diameter d, volume $v = (1/6)\pi d^3$, mass m, density $\rho = m/v$, and $y = \varepsilon/\bar{l}$ where $\bar{l} = (2/3)d$, the specific energy $z = \varepsilon/m$ becomes:

$$z = (\frac{4}{\pi d^2 \rho})y \qquad \text{Eq. 7}$$

That is, the specific dose for an event of lineal energy, y, is proportional to y and, historically, the dose distributions usually are presented with y as the independent variable rather than z. If the probability of an event with lineal energy' y is p(y), then z is proportional to yp(y). Therefore, if we plot yp(y) versus y, we have a distribution of the probability of depositing a dose d(y) = yp(y)

As we noted previously, in principle, we can quantify the fractional contribution of events (or dose) between two arbitrary values of lineal energy, y_1 to y_2, by calculating the ratio of area between y_1 and y_2 to the total area under the curve, i.e.:

$$P_{y1}^{y2} = \int_{y1}^{y2} p(y)dy / \int_0^\infty p(y)dy \rightarrow \sum_{y1}^{y2} p(y)\Delta y / \sum_0^\infty p(y)\Delta y \qquad \text{Eq. 8}$$

and

$$D_{y1}^{y2} = \int_{y1}^{y2} d(y)dy / \int_0^\infty d(y)dy \rightarrow \sum_{y1}^{y2} d(y)\Delta y / \sum_0^\infty d(y)\Delta y \qquad \text{Eq. 9}$$

(note that conventional notation in microdosimetry fails to distinguish between the variable, d, and the differential d, so, unfortunately, it is up to the reader to discern the difference from context.) For those readers who abhor equations, these simply state that the area under theses curves is the sum of the area for each histogram, i.e., the width of the histogram, y_2-y_1, times the value of its height, p(y). The dilemma we face, however, is that when we plot these data, we get data hugging both axes if we display the entire data set, as we saw in Figure 1. While the integrals still give the correct fractional contributions, it is usually impossible to relate to the results visually. To circumvent this problem, we take advantage of the fact that the derivative of the natural logarithm of a function, y, is $d(\ln y)/dy = 1/y$. Consequently:

dy =yd(ln y)=kyd($\log_{10}$ y)   Eq. 10

where k = 2.30258 because 2.30258 $\log_{10}$ y = ln y.

Substituting kyd($\log_{10}$ y) for dy and dropping the subscript for $\log_{10}$ in Equations 8 and 9 gives:

$$P_{y1}^{y2} = \int_{y1}^{y2} yp(y)d(\log y) / \int_{0}^{\infty} p(y)d(\log y) \to \sum_{y1}^{y2} yp(y)\Delta(\log y) / \sum_{0}^{\infty} yp(y)\Delta(\log y) \qquad \text{Eq. 11}$$

$$D_{y1}^{y2} = k \int_{y1}^{y2} yd(y)d(\log y) / \int_{0}^{\infty} yd(y)d(\log y) \to \sum_{y1}^{y2} yd(y)\Delta(\log y) / \sum_{0}^{\infty} yd(y)\Delta(\log y) \qquad \text{Eq. 12}$$

These equations tell us that we can plot yp(y) versus log y and the area between two values of y will still be proportional to the fractional dose in that interval. Moreover, when we do plot the
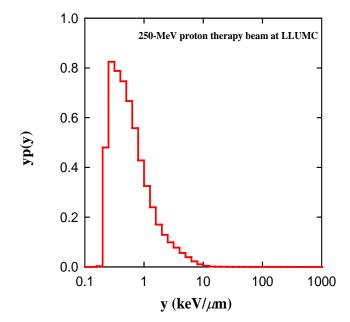

Fig. 2: The data presented as a log-linear plot in Figure 1 but replotted as yp(y) versus y. In this representation, the area under the curve between two values of y still represent the fractional contribution to the total fluence of events between those y value while the structure of the distribution is more visually apparent.
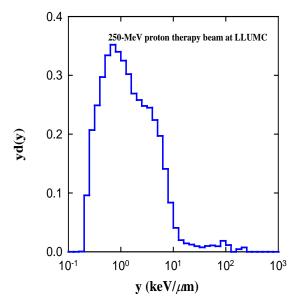

Fig. 3: A histogram of yd(y) versus y plotted semi-logarithmically where the area under the curve between two values of y is proportional to the physical dose absorbed by events in that interval. Again, this representation, rather than the linear-linear plot of d(y) versus y, provides more visual information concerning the regions' relative contributions to the total dose.

data in this manner, we get a representation that provides us with more details as demonstrated in Figures 2 and 3 for a proton beam at Loma Linda University Medical Center with a maximum energy of about 250 MeV. (Most solar protons at low Earth orbits and most trapped protons have energies below this value, while most galactic protons have higher energies (Dicello and Cucinotta, 2002).) What we see in Figure 2 in terms of the probabilities of events occurring from these primary protons is that most of the events are depositing lineal energies below 1

keV/μm with the modal y calculated to be 0.3 keV/μm, As noted previously, the shape and the relative contributions to different regions of the distribution are a function of the target size. Nevertheless, if we look at the probabilities of depositing a given amount of dose in Figure 3, some of the underlying physics mechanisms can be inferred and interpreted. For example, the majority of the dose is being contributed by events broadly distributed up to about 10 keV/μm, slightly less than the maximum lineal energy of electrons, with significant, albeit small, probabilities as high as 200 keV/μm, lineal energies greater than the maximum that could be deposited by protons. A more detailed discussion would show that such rare events, arising primarily from energetic heavy ions or alternatively short-range recoils, potentially can have significant impact on the biological consequences from such radiations [Dicello, 1992].

So far, we have limited our discussion almost entirely to protons. Let us complete the discussion by comparing event and dose distributions for some of the other major particles in space shown in Figures 4 and 5 (Dicello,Wa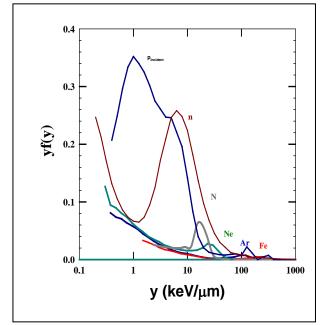siolek, M. Zaider, 1991). The dominant primary cosmic ray in terms of abundance is the proton, with primary heavy ions frequently assumed to have maximum biological effectiveness. (In these data most of the heavy-ion spectra were for equivalent average pathlengths of about 0.4 μm rather than 4/3 μm used for the proton spectra. We have added a spectrum for 14.5 MeV neutrons because high-energy neutrons are frequently a major secondary particle produced in a spacecraft, even in the astronauts themselves, both in terms of relative abundance and RBE. We see in Figure 4, as we saw with protons, a decreasing contribution for all particles with increasing lineal energies despite the high stopping powers or linear energy transfers (LETs) of these particles These most abundant events are largely the result of delta rays from the primary particles (i.e., secondary electrons traveling away from the central trajectory of the primary), some of which can travel tens of centimeters or more in tissues, as well as secondary photons and high-energy heavy secondaries. The delta-ray cont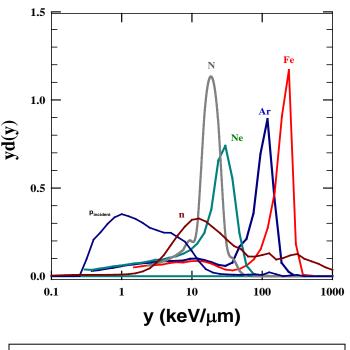ribution is related to the energy and mass (momentum) of the primary particle which, in these cases, range from about 400 to 600 MeV/nucleon. About 75-80% of the events are in this region even for the case iron with a dE/dx of about 200 keV/μm. However, these abundant events deposit little energy in comparison with the primaries, so their contribution to the dose is less, as shown in Figure 5. In this plot the area under any curve between two values of y is proportional to the fractional dose contributed by that region with all of the curves have been normalized to the same total dose. Now we see that the delta rays continue to deposit a significant dose, but it is only about 20-30% of the total dose. Again, the proton dose is largely between 0.1 and 10 keV/μm. Neutrons are particularly interesting in that

Fig. 4: *Frequency distributions for 14.5-MeV neutrons, 200-MV protons, and HZEs reported by Dicello et al., 1991 plotted semi-logarithmically. Each particle spectrum is normalized to the same total dose.*

they show little dose from delta rays, because neutrons have no charge and interact primarily via the nuclear force, but electrons have no nuclear force. Moreover, because the neutrons deposit their energy primarily by secondary charged particles, they do so over a broad region extending from about 0.3 to 1000 kev/μm. Because of this, regardless of the region of maximum sensitivity to damage of a particular tissue or organ, neutrons are depositing significant energies in that region and, therefore, tend to be very effective, which translates to high RBEs.

Microdosimetric measurements for high-energy protons and heavier ions have been available since the early 1970 and have been instrumental in reshaping both our interpretations of ground-based biological results and significantly altering early interpretations and attempts to extrapolate into space environments. As one example, these data showed the large contributions both from delta rays and secondaries to the absorbed doses in microscopic and sub-microscopic targets that led researchers [Fry and Lett, 1988; Dicello, 1992] to question some of the earlier high relative effects predicted for HZEs relative to those for protons and photons proposing values that are more in line with recent observations. (e.g.., Dicello et al., 2004;). The long lag time

Fig. 5: Dose distribution for 14.5-MeV protons, 200-MeV neutrons, and HZEs reported by Dicello et al., 1991 plotted semi-logarithmically. Each particle spectrum is normalized to the same total dose.

that sometimes occurs between the physical observations and their application to interpreting biological data can be explained in part as a result of the esoteric nature of the microdosimetric data and, therefore, unfamiliarity and perhaps disinterest with these details on the part of the biology community. If so, perhaps short reviews such as this can provide newer researchers or those with only occasional exposure with the fundamentals to better understand and use this resource.

REFERENCES

J. F. Dicello, "HZE Cosmic Rays in Space. Is It Possible That They Are Not the Major Radiation Hazard?" Radiat. Protect. Dosimetry, 44, 253-258. (1992).

Dicello J. F**.,** Christian A., Cucinotta F. A., Gridley D. S., Kathirithamby R., Mann J., Markham A. R., Moyers M. F., Novak G. R., Piantadosi S., Ricart-Arbona R., Simonson D. M., Strandberg J. D., Vazquez M., Williams J. R., Zhang Y., Zhou H., Huso D., "In vivo mammary tumourigenesis in the Sprague-Dawley rat and microdosimetric correlates." Phys Med Biol. 49, 3817-30 (2004).

J. F. Dicello and F. A. Cucinotta, "Space Radiation" in Encyclopedia of Space Science and Technology, H. Mark, Ed.: John Wiley & Sons, Inc., Hoboken, NJ, 2002.

J. F. Dicello, M. Wasiolek, and M. Zaider, "Measured Microdosimetric Spectra of Energetic Ion Beams of Fe, A, Ne, and C: Limitations of LET Distributions and Quality Factor in Radiation Effects and Space Research." IEEE Trans. Nucl. Scien. 38, 1203-1209 (1991).

Fry, RJM, and Lett, J. T., "Radiation Hazards in Space put in Perspective." Nature 335, 305-306 (1988).

Letaw, J.R., Silberberg, R., and Tsao, CH, "Radiation Hazards on Space Missions." Nature, 330, 709-710 [1987].

National Council on Radiation Protection and Measurements,"Fluence-Based and Microdosimetric Event-Based Methods for Radiation Protection in Space." NCRP Report No. 137, Bethesda, MD (2001)

Proceedings of the 15th International Symposium on Microdosimetry: Radiat Prot Dosimetry. 2011 Feb;143(2-4) and published proceedings of earlier symposiums]

M. Zaider and J. F. Dicello, "Microdosimetry and Its Medical Applications," Chapter 18, pp. 544-550: Charged Particle and Photon Interactions with Matter," A. Mozumder and Y. Htano, eds., Marcel Dekker, Inc., New York 2004 and references therein.